Current Biology 24, 1176–1186, June 2, 2014 ©2014 Elsevier Ltd All rights reserved http://dx.doi.org/10.1016/j.cub.2014.04.033

Article

# A SUF Fe-S Cluster Biogenesis System in the Mitochondrion-Related Organelles of the Anaerobic Protist *Pygsuia*

**Courtney W. Stairs,[1,2] Laura Eme,[1,2] Matthew W. Brown,[3,4] Cornelis Mutsaers,[1,2] Edward Susko,[1,5] Graham Dellaire,[2,6] Darren M. Soanes,[7] Mark van der Giezen,[7] and Andrew J. Roger[1,2,*]**

[1]Centre for Comparative Genomics and Evolutionary Bioinformatics, Dalhousie University, Halifax, NS B3H 4R2, Canada

[2]Department of Biochemistry and Molecular Biology, Dalhousie University, Halifax, NS B3H 4R2, Canada

[3]Department of Biological Sciences, Mississippi State University, Mississippi State, MS 39762, USA

[4]The Institute for Genomics, Biocomputing, and Biotechnology, Mississippi State University, Mississippi State, MS 39762, USA

[5]Department of Mathematics and Statistics, Dalhousie University, Halifax, NS B3H 4R2, Canada

[6]Department of Pathology, Dalhousie University, Halifax, NS B3H 4R2, Canada

[7]Biosciences, University of Exeter, Exeter EX4 4QD, UK

## Summary

**Background:** Many microbial eukaryotes have evolved anaerobic alternatives to mitochondria known as mitochondrion-related organelles (MROs). Yet, only a few of these have been experimentally investigated. Here we report an RNA-seq-based reconstruction of the MRO proteome of *Pygsuia biforma*, an anaerobic representative of an unexplored deep-branching eukaryotic lineage.

**Results:** *Pygsuia*'s MRO has a completely novel suite of functions, defying existing "function-based" organelle classifications. Most notable is the replacement of the mitochondrial iron-sulfur cluster machinery by an archaeal sulfur mobilization (SUF) system acquired via lateral gene transfer (LGT). Using immunolocalization in *Pygsuia* and heterologous expression in yeast, we show that the SUF system does indeed localize to the MRO. The *Pygsuia* MRO also possesses a unique assemblage of features, including: cardiolipin, phosphonolipid, amino acid, and fatty acid metabolism; a partial Kreb's cycle; a reduced respiratory chain; and a laterally acquired rhodoquinone (RQ) biosynthesis enzyme. The latter observation suggests that RQ is an electron carrier of a fumarate reductase-type complex II in this MRO.

**Conclusions:** The unique functional profile of this MRO underscores the tremendous plasticity of mitochondrial function within eukaryotes and showcases the role of LGT in forging metabolic mosaics of ancestral and newly acquired organellar pathways.

## Introduction

Mitochondria of modern-day eukaryotes evolved from an $\alpha$-proteobacterial endosymbiont that was integrated as an organelle within a host cell prior to the last eukaryotic common ancestor [1]. In aerobic eukaryotes, mitochondria carry out a number of important functions, including pyruvate decarboxylation, oxygen-dependent ATP production, amino acid metabolism, and iron-sulfur (Fe-S) cluster biosynthesis. Over the past 20 years, investigations into the mitochondria or homologous organelles of anaerobic organisms (mitochondrion-related organelles, MROs) have revealed a variety of different metabolic phenotypes.

Classical "aerobic" mitochondria generate ATP by oxidative phosphorylation using ATP synthase coupled to the electron transport chain, ultimately reducing $O_2$ to $H_2O$. However, anaerobically functioning mitochondria have also been described in a number of eukaryotes (e.g., *Ascaris*) that, under hypoxic conditions, produce ATP but employ a terminal electron acceptor instead of $O_2$ (e.g., fumarate [2]). Radically different MROs known as hydrogenosomes, which are found in protist parasites such as *Trichomonas*, lack organellar genomes and produce ATP by an anaerobic pathway that is typically not found in classical mitochondria. In these organelles, pyruvate is oxidized to acetyl-CoA and $CO_2$ by a pyruvate:ferredoxin oxidoreductase (PFO), and the reduced ferredoxin is reoxidized by an iron-only [FeFe] hydrogenase that reduces protons to $H_2$ gas [3]. Acetyl-CoA is then converted to acetate by an acetate:succinate CoA transferase (ASCT), and the resulting succinyl-CoA is utilized by succinyl-CoA synthetase (SCS) to generate ATP by substrate-level phosphorylation [4]. Other anaerobic protists contain MROs called mitosomes that do not produce ATP and that typically function in Fe-S cluster formation via a mitochondrial-type iron-sulfur cluster (ISC) system (e.g., *Giardia* [5]). In mitosome-containing protists such as *Giardia* and *Entamoeba*, ATP-production occurs by substrate-level phosphorylation in their cytoplasms [6].

Recent investigation of hitherto neglected parasitic, commensal, and free-living organisms has greatly expanded the spectrum of known functions of MROs [7–11]. For example, several distantly related protists have organelles recently described as "hydrogen-producing mitochondria" (HPMs). HPMs not only have mitochondrial genomes and many canonical mitochondrial pathways (including components of the electron-transport chain, ETC), but also possess enzymes of the anaerobic "hydrogenosomal" ATP generation pathway. Other MROs lacking mitochondrial DNA have also been described, each with a distinct combination of mitochondrial and hydrogenosomal properties. For instance, the MROs of the free-living excavate *Trimastix pyriformis* possess several mitochondrial pathways involved in amino acid metabolism, as well as enzymes for hydrogen and anaerobic ATP production, and lack full ETC complexes [10, 12]. In contrast, *Mastigamoeba balamuthi*, a free-living amoeba, has MROs with complex II (but no other ETC complexes) in addition to serine and glycine metabolic pathways, as well as a [FeFe] hydrogenase and a PFO [7].

Virtually all mitochondria and MROs of all studied extant eukaryotes generate Fe-S clusters for mitochondrial Fe-S proteins using the ISC system [13]. Fe-S clusters can also be synthesized in other cellular compartments such as the cytosol or in plastids. The cytosolic iron-sulfur cluster

*Correspondence: andrew.roger@dal.ca

assembly (CIA) machinery matures cytoplasmic and nuclear Fe-S proteins and, in yeast, has been show to rely on the ISC system to supply it with an unknown sulfurous factor, so-called "factor X" [13]. Plastids use an endosymbiont-derived sulfur mobilization (SUF) pathway [14].

However, several eukaryotes have recently been shown to deviate from the foregoing patterns. *Entamoeba* and *Mastigamoeba* completely lack the ISC system and instead employ a nitrogen-fixation (NIF)-related Fe-S biogenesis system that they have acquired by lateral gene transfer (LGT) from ε-proteobacteria [15, 16]. In *Mastigamoeba*, there are duplicates of the *nif* genes that encode distinct paralogs that function in the cytosol and the MROs of this organism [15]. The only other known exception to the general eukaryotic pattern is in the anaerobic stramenopile *Blastocystis* sp., in which an archaeal-like SUFCB fusion protein was shown to function in the cytosol and is induced under oxidative stress [17].

Here, we reconstruct the proteome of the MROs of the breviate *Pygsuia biforma*, a free-living aerotolerant anaerobic amoeboid flagellate from hypoxic marine sediments [18]. The breviates have recently been shown to be an early emerging group, branching at the base of the eukaryote supergroup Obazoa, comprised of animals and fungi (Opisthokonta) and Apusomonads [18]. Our predictions reveal an extraordinarily distinct MRO in this organism. In addition to possessing several systems and pathways never before detected in MROs (e.g., rhodoquinone, cardiolipin, and phoshonolipid biosynthesis), it has hydrogenosomal-like anaerobic energy metabolism and a partial electron transport chain consisting of complex II, alternative oxidase (AOX), and electron transferring flavoprotein (ETF). Most unexpectedly, a mitochondrial-type ISC system appears to be completely absent. Instead, *Pygsuia* expresses duplicated methanomicrobiales/*Blastocystis*-like SUFCB proteins that it has acquired by LGT. One of the SUFCB proteins localizes to its MRO, suggesting that it may functionally replace the ISC system. This is only the second known lineage where the mitochondrial ISC system has apparently been lost and the first case where the SUFCB system seems to have taken over its role in Fe-S cluster biogenesis within MROs.

## Results

### Metabolic Pathway Prediction in *Pygsuia biforma* and *Breviata anthema*

From the filtered transcriptomic data set, a total of 122 proteins were putatively predicted to be localized to the MRO matrix (MM), inner membrane (IM), intermembrane space (IMS), or outer membrane (OM) of *Pygsuia* on the basis of homology to known mitochondrial proteins inferred from Mitominer [19] and/or Mitoprot and TargetP prediction scores (>0.5) for mitochondrial targeting signals (MTSs; Document S2) [20, 21]. The vast majority (71/76) of MM proteins have N-terminal MTSs, whereas only half of the IM/IMS proteins have one (22/43). None of the OM proteins have an MTS (0/3), as expected. In addition, visual inspection of these putative *Pygsuia* sequences allowed us to identify a characteristic thymidine-rich pattern in the 5′ untranslated region (UTR). RNA sequencing (RNA-seq) coverage information, MTS statistics, and gene and UTR sequences can be found in Document S2.

For the Sanger EST project of *Breviata anathema*, a total of 6,937 sequences were assembled into 1,520 clusters. Genes from *Pygsuia* were used to detect the corresponding *Breviata* orthologs summarized in Document S2. We also searched the recent 454 pyrosequencing transcriptome of another closely related breviate, *Subulatomonas tetraspora* [22], using the *Pygsuia* homologs as queries (Document S2). Due to the low sequence coverage and protein complement identified in the *Breviata anathema* and *Subulatomonas tetraspora* data, the *Pygsuia* MRO protein predictions are the primary focus of this study. A metabolic reconstruction of the various MRO pathways in *Pygsuia* is shown in Figure 1. Below, we discuss the major pathways and processes that we identified, including those involved in pyruvate and ATP generation, protein import and processing, Fe-S cluster biogenesis, amino acid and lipid metabolism, and small-molecule transport. For key proteins, we examine the subcellular localization using heterologous expression in yeast and immunofluorescence microscopy.

### Pyruvate and Energy Metabolism

Glycolysis-derived pyruvate is typically imported into mitochondria via the recently identified pyruvate carrier MCP1/MCP2 (brain protein 44) [23]. However, pyruvate can also be generated from malate via malic enzyme (ME) [24]. Two putatively organellar $NAD^+$- and $NADP^+$-dependent MEs were identified in *Pygsuia*, ME1 and ME2, respectively. In mitochondria and some HPMs, this pyruvate is typically oxidized via the pyruvate dehydrogenase complex (PDC) [25]. However, in other MROs, acetyl-CoA is generated by a pyruvate:ferredoxin oxidoreductase (PFO), a single-subunit enzyme proposed to have been acquired by LGT [26]. In *P. biforma*, we detected four transcripts encoding putative pyruvate oxidation enzymes: two PFOs with predicted MTS (*Pb*-mPFO1 and *Pb*-mPFO2), one PFO without MTS (*Pb*-cPFO), and one PNO without MTS (*Pb*-cPNO). Maximum-likelihood (ML) and Bayesian phylogenetic analyses indicate that all breviate sequences emerge within a monophylyetic eukaryotic grouping (bootstrap support [BV] = 70%; posterior probability [PP] = 0.99). Although there is little resolution in the placement of the breviate sequences within the eukaryotic clade, at least two PFO copies appear to have been established in breviates before the divergences of *P. biforma* and *B. anathema* (i.e., *Ba*-PFOa and *Ba*-PFOb group with *Pb*-mPFO1, and *Ba*-PFOc groups with *Pb*-cPFO1) (Document S3). Curiously, *Pygsuia* also encodes homologs of the eukaryotic pyruvate:formate lyase (PFL) and activating enzyme, another anaerobic enzyme catalyzing the conversion of pyruvate to acetyl-CoA sometimes found in MROs [27–29]. The lack of a targeting peptide is suggestive of a cytosolic localization in *Pygsuia*.

In hydrogenosomes, the reduced ferredoxin generated by PFO is typically reoxidized by an [FeFe] hydrogenase (HYDA) generating molecular hydrogen [30]. We identified genes encoding full-length and partial canonical HYDA (*Pb*-mHYDA and Pb-HYDA4) in *P. biforma* and one (incomplete) copy in *B. anathema* (*Ba*-HYDA). In addition, we found four other putative HYDA-like proteins in *P. biforma* possessing several distinct domain architectures, including three with C-terminal flavodoxin (CYSJ) domains (*Pb*-cHYDA-CYSJ1 to *Pb*-cHYDACYSJ3) and one with an N-terminal sulfide dehydrogenase (*Pb*-cSD-HYDA). Of these six proteins, only *Pb*-mHYDA has a predicted MTS, suggesting that the other HYDA-like proteins are nonorganellar. Phylogenetic analyses, although poorly supported in general, indicate that the canonical and noncanonical HYDAs of the breviates branch among other eukaryotic sequences, with only *Pb*-cHYDA-CYSJ1 and *Pb*-cHYDA-CYSJ2 grouping together strongly (Document

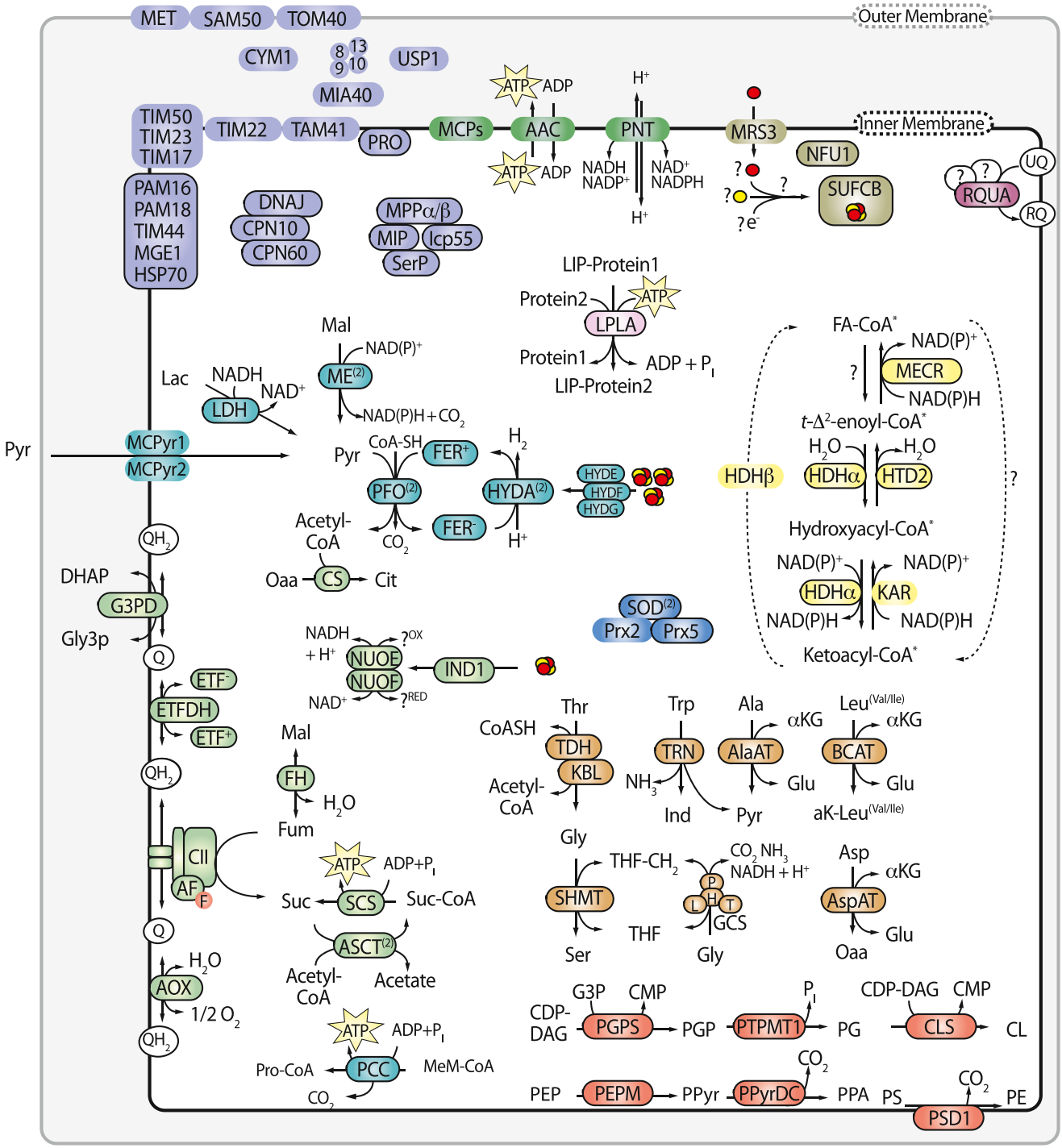


Figure 1. Predicted MRO Metabolism of Selected *Pygsuia biforma* Proteins Determined by BLAST-Mediated Homology Probing

Sequences with predicted N-terminal MTS are outlined in black. Unknown proteins are shown with a question mark. Red and yellow circles represent iron and sulfur, respectively. *Protein import and folding (purple)*: Met, Metaxin; SAM50, sorting assembly machinery 50 kDa; TOM, translocator of the OM; CYM1, presequence protease; TIM8, TIM9, TIM10, and TIM13, tiny translocator of the IM 8, 9, 10, and 13, respectively; UPS1, IMS chaperone/slowmo protein; TAM41, translocator assembly and maintenance protein 41; PRO, Prohibitin; PAM, presequence translocase-associated motor; MGE1, mitochondrial GRPE protein; CPN, chaperonin; HSP, heat shock protein; MPP, mitochondrial processing peptidase; MIP, mitochondrial intermediate peptidase; and SerPr: serine protease. *Carriers (dark green)*: MCPs, mitochondrial carrier proteins; AAC, ATP:ADP carrier protein; and PNT, pyridine nucleotide transhydrogenase. *Fe-S cluster biosynthesis (brown)*: SUFCB, sulfur mobilization C/B fusion; NFU1: NifU-like protein; and MRS3: $Fe^{2+}$ carrier. *Rhodoquinone biosynthesis (dark pink)*: UQ, ubiquinone; RQ, rhodoquinone; and RQUA, RQ methyltransferase. *Lipoate metabolism (light pink)*: LIP, lipoate; and LPLA, lipoate-protein ligase. *Pyruvate metabolism (blue)*: MCPyr1/MCPyr2, mitochondrial pyruvate carrier 1/2 (brain protein 44); Lac, lactate; LDH, lactate dehydrogenase (DH); Mal, malate; ME, malic enzyme(s); Pyr, pyruvate; FER, ferredoxin; PFO, Pyr:fer oxidoreductase (OR); HYDA, [FeFe] hydrogenase; and Hyde-G, HYDA maturases. *TCA cycle and electron transport (light green)*: CS, citrate synthase; OAA, oxaloacetate; NUOE/F, NADH:UQ OR; IND1, Fe-S protein required for NADH DH; FUM, fumarate; FH, fumarate hydratase; SUC, succinate; CII, succinate DH/complex II; AF, CII assembly factor; F, flavin; SCS, succinyl-CoA

*(legend continued on next page)*

S3). All three HYDA maturases (HYDE, HYDF, and HYDG) responsible for proper assembly of the H-cluster of HYDA [31] were identified in single copy with predicted MTSs. For each of the three HYDA maturases, the monophyly of eukaryotic homologs was recovered in ML and Bayesian phylogenetic analyses with moderate to maximum support (Document S3; HydE, BP = 47, PP = 0.99; HydF, BP = 100, PP = 1; HydG, BP = 99, PP = 1).

A modified tricarboxylic acid (TCA) cycle was identified in *P. biforma*, including citrate synthase, succinyl-CoA synthetase (SCS$\alpha$/$\beta$), succinate dehydrogenase/complex II (CII; SDHA-D, and SDH assembly factor 2), fumarate hydratase (FH), and propionyl-CoA carboxylase (PCC$\alpha$/$\beta$). However, aconitase, isocitrate dehydrogenase, $\alpha$-ketoglutarate dehydrogenase, and an organellar malate dehydrogenase were not identified. The absence of these enzymes suggests that malate might ultimately be converted to succinate. In this scenario, CII would be functioning in reverse as a fumarate reductase (FRD), and the FRD-derived succinate is used as a CoA acceptor (from acetyl-CoA or propionyl-CoA) by acetate:succinyl-CoA transferase (ASCT), an enzyme often found in anaerobic mitochondria, HPMs, and hydrogenosomes. We identified two putative ASCTs in *P. biforma*, one corresponding to each of the subtype 1B and 1C families, both with predicted MTSs. The succinyl-CoA presumably generated by these enzymes is used by the TCA cycle enzyme SCS to generate ATP/GTP by substrate-level phosphorylation, as is the case in *Trichomonas* [4].

Unlike the above-mentioned TCA cycle enzymes that are of mitochondrial provenance, the phylogenetic affinities of ASCT are less clear [4]. For this reason, we conducted phylogenetic analyses of the *P. biforma* ASCT-1B and ASCT-1C homologs. The ASCT-1C ML tree shows a poorly supported eukaryotic clade within which *Pb*-ASCT-1C branches weakly as a sister group to two trichomonad homologs (Document S3); one of these—the enzyme from *T. vaginalis*—has been experimentally characterized [4]. In the ASCT-1B phylogeny, *P. biforma* emerges from within a grouping of eukaryotic sequences, but the precise branching order of the tree is not well supported (Document S3).

The presence of genes encoding putatively MRO ubiquinone-utilizing (UQ) enzymes such as alternative oxidase (AOX), SDH/FRD, electron-transferring flavoprotein dehydrogenase (ETFDH), NAD(P)H dehydrogenase (NQO1), and glycerol-3-phosphate dehydrogenase (G3PDH) prompted a search for a quinone biosynthesis pathway. Only geranylgeranyl transferase (ISPA) and coenzyme Q methylase-like protein (COQ5) were identified, each without a MTS. While AOX and G3PD are known to use UQ as their electron acceptor [32, 33], CII has been shown to use rhodoquinone (RQ) when functioning as a FRD [34]. The exact pathway of RQ biosynthesis is unknown; however, recent reports have demonstrated that in *Rhodospirillum rubrum*, RQ is synthesized from UQ via a number of reactions, one of which is catalyzed by a putative methyltransferase (RQUA) [35, 36]. Unexpectedly, we identified a homolog of RQUA in *Pygsuia* that possesses a MTS, suggesting that RQ is synthesized in its MRO. A survey of the *nr* database revealed that a number of other eukaryotic lineages have RQUA homologs, including obligate (*Blastocystis*) and facultative (*Euglena*) anaerobes, the latter of which is known to synthesize RQ [37]. Phylogenetic analysis of RQUA indicates a patchy and limited distribution in a small number of $\alpha$-proteobacteria, and $\beta$-proteobacteria, and eukaryotes. The extremely limited distribution of this enzyme within eukaryotes coupled with the atypical phylogenetic groupings observed (Figure 2) strongly suggests the enzymes have been acquired multiple times by eukaryotes via LGT from distinct bacterial or eukaryotic donors.

The only other respiratory complex we identified was the two soluble subunits of NADH:ubquinone oxidoreductase (NUOE and NUOF) from complex I, along with the putative assembly factor (IND1/MRP1-like). These two subunits of NUO are often found in hydrogenosomes of protists and are presumed to function in a Q-independent electron transfer reactions [38].

### *Pygsuia* MROs Contain Canonical Protein Import and Processing Machinery

Mitochondrial genes encoded on the nuclear genome are recognized and imported to the MM or IMS via the protein import machinery. In *Pygsuia*, we identified two components of the translocator of the outer mitochondrial matrix complex (TOM40 and SAM50), all four tiny translocators of the inner mitochondrial membrane (TIM8, TIM9, TIM10, and TIM13), IMS import and assembly protein 40 (MIA40), IMS sorting protein (UPS2), TIM22, the majority of the TIM23 and presequence translocase-associated motor complex (PAM) complex (TIM50, TIM23, TIM17, HSP70, MGE1, TIM44, PAM16, and PAM18), an assembly and maintenance factor for the translocator machinery (TAM41), chaperonins (CPN10 and CPN60), and membrane integrity protein prohibitin (PRO/PHB). MTSs were identified for all matrix-associated import proteins, and internal Mia40 targeting sequences [39] were identified for IMS proteins TIM9 and TIM10 (data not shown). A variety of proteases and processing peptidases were also identified, including presequence peptidase (CYM1), serine protease (SERPr), and mitochondrial processing peptidase (MPP$\alpha$ and MPP$\beta$), responsible for cleaving the N-terminal presequence of mitochondrial proteins after import into the organelle. We used sequence logo analysis to graphically represent the level of conservation of the predicted MTS and observed the typical features, including arginine or lysine in the penultimate position [20, 21] (Figure S1). There was also a preference for leucine or phenylalanine immediately following the methionine (Figure S1).

synthetase; ASCT; acetate:succinyl-CoA transferase(s); DHAP; dihydroxyacetone phosphate; Gly3p, glycerol-3-phosphate; G3PD, Gly3p DH; ETF, electron transferring flavoprotein; AOX, alternative oxidase; and Q/$QH_2$, quinone/quinol. *Fatty acid metabolism (yellow)*: FA, fatty acid; MECR, mitochondrial trans-2-enoyl-CoA reductase; HTD2, 3-hydroxyacyl thioester dehydratase 2; KAR, ketoacyl reductase; and HDH$\alpha$/HDH$\beta$, trifunctional enzyme, hydroxyacyl DH; and *, acyl-carrier protein is used in place of CoA during biosynthesis. *Amino acid metabolism (light brown)*: Thr, threonine; TDH, Thr DH; KBL, keto-butyrate lyase; Trp, tryptophan; TRN, tryptophanase; Ind, indole; Gly, glycine; Ala, alanine; ALAT, ala amino transferase (AT); Leu, leucine; Val, valine; Ile, isoleucine; $\alpha$-KG, $\alpha$-ketoglutarate; Glu, glutamate; SHMT, serine hydroxymethyl transferase; GCS, glycine cleavage system (P, H, L, T); Ser, serine; THF, tetrahydrofolate; and Asp, aspartate. *Oxidative stress (dark blue)*: SOD, superoxide dismutase; Prx2, peroredoxin; and Prx5, peroxidase. *Lipid metabolism (orange)*: CDP-DAG, cytidine diphosphate diacylglycerol; PGPS, CDP-DAG-glycerol-3-phosphate 3-phosphatidyltransferase; PGP, phosphatidylglycerol phosphate; PG, phosphatidylglycerol; PTPMT1, protein-tyrosine phosphatase mitochondrial 1; CL, cardiolipin; CLS, CL synthase; CMP, cytidine monophosphate; PEP, phosphoenolpyruvate; PEPM, PEP mutase; PPyr, phosphonopyruvate; PPyrDC, PPyr decarboxylase; and PSD1, phosphotidylserine decarboxylase 1. See also Document S2.

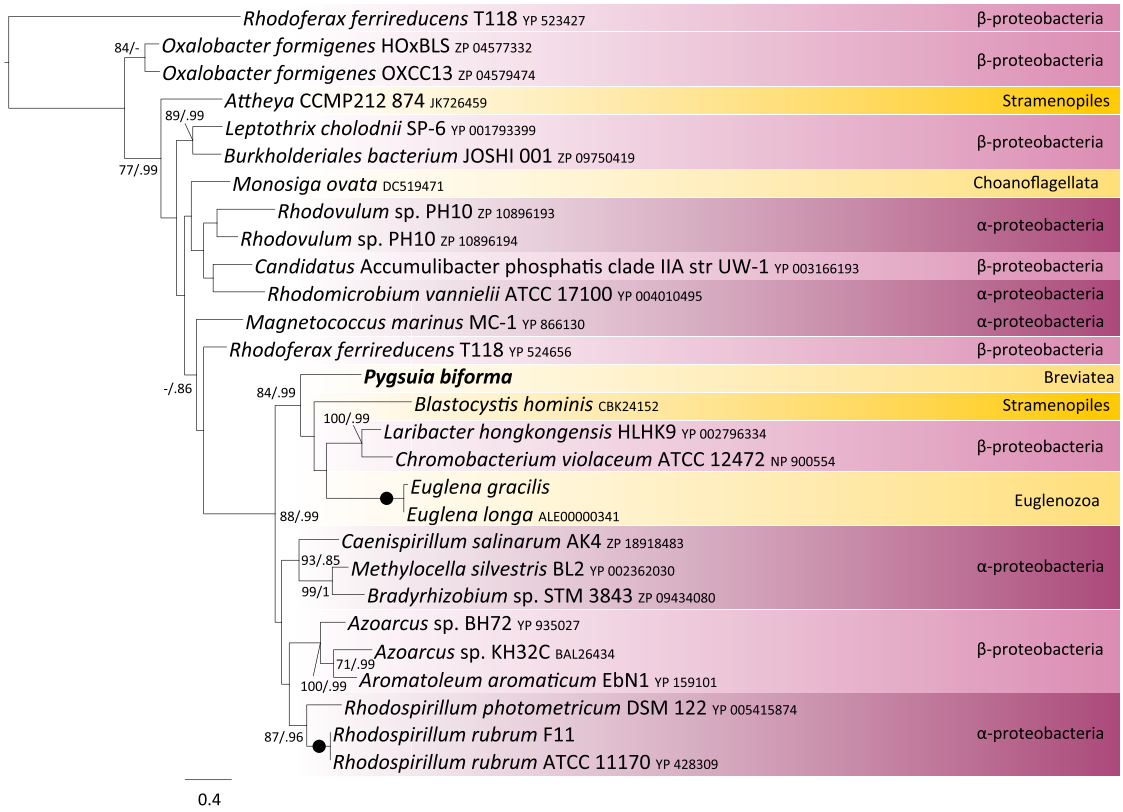


Figure 2. Phylogeny of RQUA Homologs

Maximum-likelihood (ML) tree of RQUA (28 sequences and 193 sites) rooted with UBIE/COQ5 methyltransferase from *Rhodoferax ferrireducens*. Bootstrap support (BV) and posterior probability (PP) values for each branch were calculated using RAxML and PhyloBayes. Only BV and PP values greater than 50% and 0.5 are shown. Branches with maximum support (BV = 100%; PP = 1.0) are depicted with black circles. Pink and yellow shading represent Proteobacteria and Eukaryotes, respectively. See also Document S3.

## Fe-S Cluster Biogenesis

All eukaryotes studied to date, with the exception of *E. histolytica* [16] and *M. balamuthi* [7, 15], utilize the mitochondrial ISC system for mitochondrial/MRO Fe-S cluster biogenesis. Considering this, the most intriguing result from the *P. biforma* RNA-seq data was the apparent absence of the vast majority components of the ISC machinery (i.e., ISCA, ISCU, Frataxin, ISPG/H, ISCR, YAH1, and ARH1) and their associated proteins involved in factor X transport and iron homeostasis (ERV1, ATM1/ABC7, or ABCB6/MtABC3 proteins) [40]. As factor X is thought to be indispensable for the function of CIA-mediated cytoplasmic Fe-S cluster assembly, the lack of the CIA components predicted to interact with factor X (i.e., the TAH18/DRE2 complex) correlates with the absence of its transporters. However, we identified all of the remaining components of the CIA system (CIA1, NPB35, CFD1, NAR1, CIA2, and MET18; data not shown).

Despite the absence of all other ISC components in *Pygsuia*, we identified a fused protein containing an ISCS-like domain fused downstream of a 4-thiouridine biosynthesis protein (ThiI). The lack of a predicted MTS on this protein, as well as its distinct evolutionary origin from mitochondrial ISCS homologs of other eukaryotes, suggests that it is unlikely to be involved in Fe-S cluster biogenesis in the MROs of *Pygsuia* (see the Supplemental Results for detailed analyses and discussion of this point).

Apart from the ISCS-like sequence, the only other putative dedicated ISC components identifiable in *P. biforma* are NFU1 and IND1. Both proteins possess canonical MTS and are phylogenetically related to other eukaryotic mitochondrial homologs (Document S3 and data not shown). In contrast, in *Breviata*, we identified the Fe-S scaffold of the ISC system (ISCU) in addition to IND1.

Although we could not identify core ISC system orthologs in *Pygsuia*, we did find two putative homologs of the SUF system in the form of a SUFCB fusion protein. Unexpectedly, one of the two SUFCB homologs (*Pb*-mSUFCB) possesses a MTS, suggesting that it functions within the MRO. The other homolog, *Pb*-cSUFCB, lacks the putative MTS. As this fusion of SUFC and SUFB is only observed in *Blastocystis* sp. and *Pygsuia*, we performed separate phylogenetic analyses of SUFB and SUFC regions and their respective prokaryotic homologs (Document S3). The two analyses resolved broadly congruent phylogenies, reflecting similar evolutionary histories of the two proteins. To improve the signal, we analyzed a concatenation of the two data sets (Figure 3). Unexpectedly, the two *Pygsuia* copies form a clade that branches with the *Blastocystis* SUFCB with maximal support (BV = 100%; PP = 1.00). This group of fused SUFCB proteins emerges as sister to homologs from Methanomicrobiales (a division of Euryarchaea), with maximal support. The close relationship between *Pygsuia* SUFCBs and *Blastocystis* homologs suggests that they descend from a unique fusion event (although there is no obvious similarity between these sequences in the fusion region). Nevertheless, their common ancestry is supported by the existence of an insertion in the

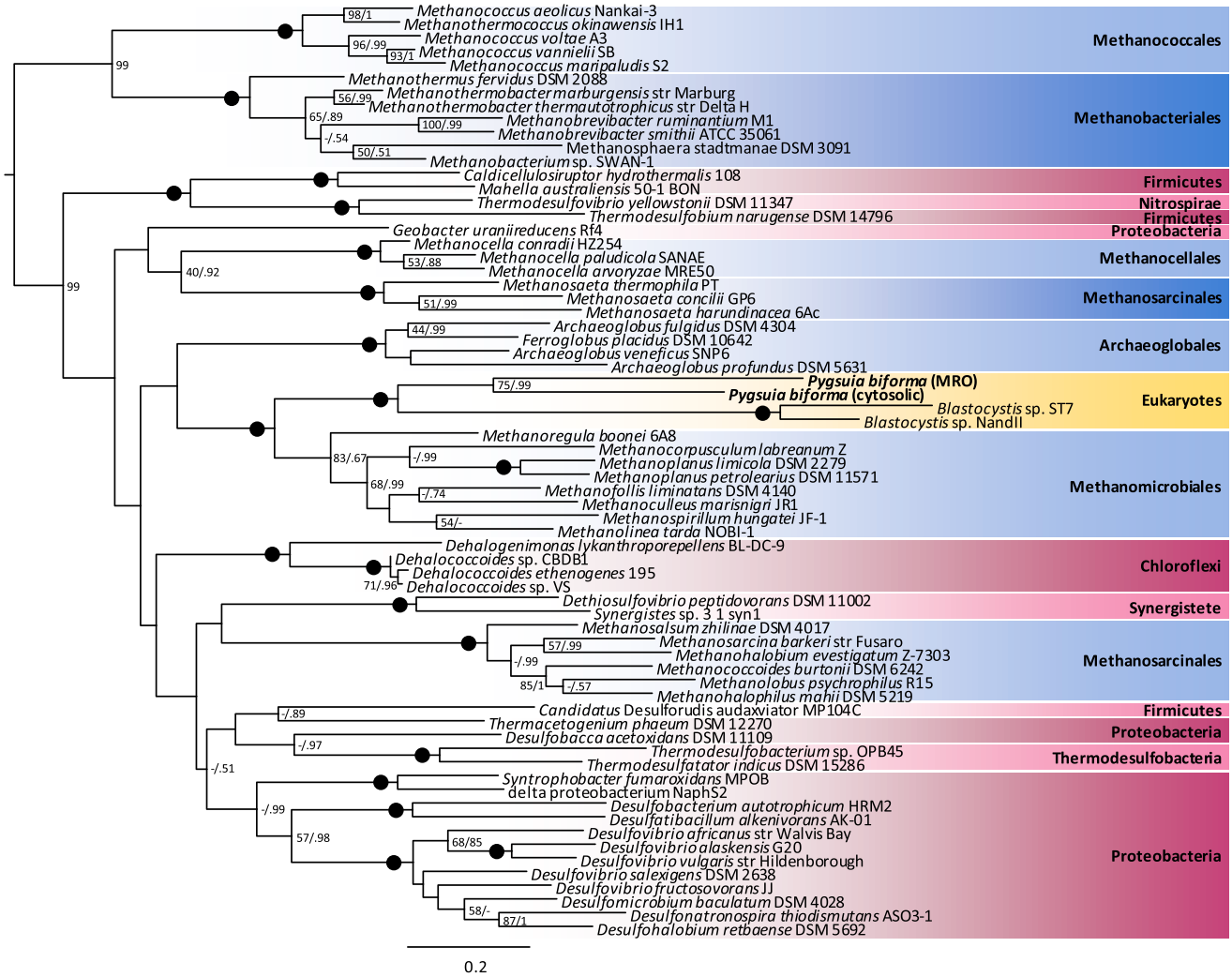


Figure 3. Phylogeny of Concatenated SUFC and SUFB Homologs

ML tree of concatenated SUFC and SUFB (68 sequences and 496 sites). The tree is rooted as shown by preliminary analyses that included a larger number of homologs. Branch labels are as described in Figure 2. Shades of blue, pink, and yellow represent various lineages of Archaea, Bacteria, and Eukaryotes respectively. See also Figure S3 and Document S3.

SUFB region shared between the *Pygsuia* and *Blastocystis* sequences to the exclusion of all closely related sequences (Figure S3). The *Pygsuia* and *Blastocystis* SUFB domains and all of their close homologs lack the $FADH_2$-binding motif that exists in the *Escherichia coli* homolog. The *Pygsuia* SUFC sequences possess the functionally important residues for metal binding and ATPase activity (including the Walker A/P loop and Walker B and D loop motifs [41]). There is also a $CX_nCX_2C$ motif toward the C-terminal part of SUFC shared only by *Blastocystis* and close prokaryotic homologs (data not shown).

### Solute Transport, Amino Acid, and Lipid Metabolism

We identified transcripts in *Pygsuia* encoding a variety of solute transporters, including 16 mitochondrial carrier proteins (MCPs) and an ADP/ATP carrier. Although we were unable to identify any of the proton-pumping respiratory complexes, we did identify two proteins that could be important for generating a proton gradient: LETM1 (a putative $Ca^+_{in}/H^+_{out}$ antiporter [42]) and pyridine nucleotide transhydrogenase (PNT; responsible for the interconversion of NADH/$NADP^+$ to $NAD^+$/NADPH with the concomitant export of protons [43]).

Enzymes responsible for the synthesis and catabolism of amino acids such as glycine, serine, threonine, tryptophan, alanine, leucine, isoleucine, and valine were identified (Figure 1). Elements of biosynthesis and β-oxidation of fatty acids were identified; however, two components do not have predicted MTS (HDHβ and KAR) (Figure 1, no outline). Furthermore, there was no evidence for a fatty acyl-CoA dehydrogenase (responsible for the formation of the enoyl-CoA moiety) or a carnitine shuttle (responsible for fatty acid transport from the cytoplasm to the MRO). We identified enzymes involved in folate biosynthesis (folylpolyglutamate synthase) and various other reactions (short-chain dehydrogenase, glutathione amine-dependent peroxidase, and acyl-CoA synthetase), each with putative MTSs reported in Document S2.

Finally, we identified a complete cardiolipin biosynthesis pathway that was recently suggested to be absent in amitochondriates [44]. Furthermore, we identified enzymes for

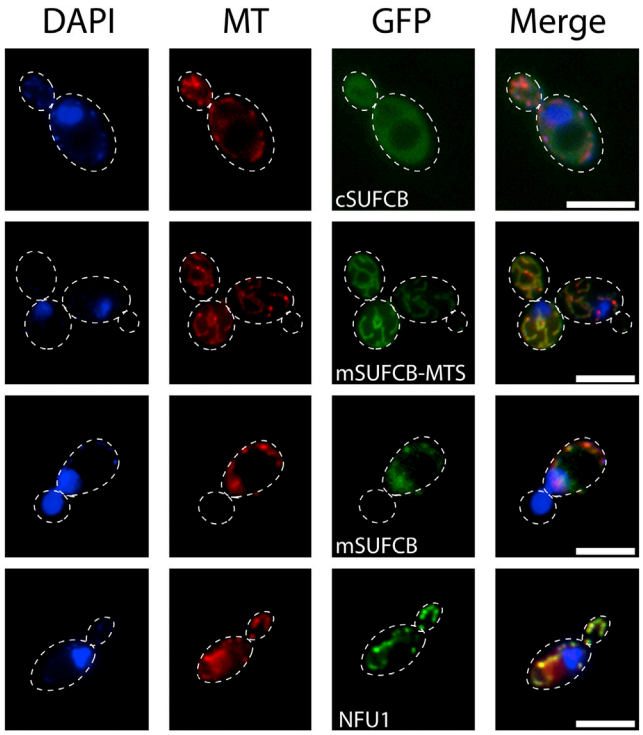


Figure 4. Localization of *Pygsuia* cSUFCB, mSUFCB, mSUFCB-MTS, and NFU1 GFP Fusion Proteins in Yeast

Indicated GFP fusion proteins were expressed in yeast (green). Mitochondria and nucleic acid were costained with MitoTracker Orange and DAPI, respectively. Scale bars represent 5 μm.

the synthesis of phosphotidylethanolamine and 2-amino-3-phosphonic acid (2-AEP), a head group for phosphonolipids. The latter pathway is rare in eukaryotes, having only been documented in mollusks, trypanosomes, and ciliates [45–48]. In *Tetrahymena*, phosphoenol pyruvate (PEP) is converted to 3-phosphonopyruvate (PPyr) by a PEP mutase (PEPM) and is subsequently converted to phosphonoacetyldehyde (PPA) by a PPyr decarboxylase (PPYRDC); both of these enzymes are present in the mitochondrial proteome [49]. The final step in the pathway is performed by a putative PPA transaminase, which does not appear to be organellar in *Tetrahymena*. In *Pygsuia*, we identified transcripts encoding all three enzymes, and, as in *Tetrahymena*, only PEPM and PPYRDC possess predicted MTSs.

We examined the evolutionary history and predicted cellular localization of PEPM, PPYRDC, and PPA transaminase across eukaryote diversity. We found homologs within Amoebozoa, the Stramenopile-Alveolata-Rhizaria (SAR) clade, Holozoa, and Kinetoplastida, although not all species have all three enzymes (Document S3). Only some of these homologs have predicted MTS. The remaining members of these eukaryote groups lack these enzymes. In phylogenetic analyses, *Pygsuia* homologs of PEPM and PPA transaminase cluster with other eukaryotic sequences, whereas its PPYRDC homolog branches separate from other eukaryotes with a heterogeneous collection of prokaryotes (see Document S3). Eukaryotic homologs of these enzymes do not have α-proteobacterial affinities that would indicate a mitochondrial origin. For a detailed discussion of these phylogenies, see the Supplemental Results.

### Localization and Morphology Studies of *Pygsuia biforma* Proteins in Yeast and In Vivo

To assess the localization of putative MRO proteins in the absence of a genetic system in *Pygsuia*, we expressed several MRO proteins fused to GFP in yeast. GFP fusion protein constructs of NIFU-like protein (NFU1), the putative targeting peptide (mSUFCB-MTS), and the full-length mSUFCB localized to the mitochondrion of yeast, whereas cSUFCB was cytosolic (Figure 4). Note that the full-length mSUFCB-GFP appears to alter the morphology of the yeast mitochondria when expressed for more than 1 hr.

Antibodies raised against a peptide specific to *Pb*-mSUFCB recognized recombinant mSUFCB (α-mSUFCBpep; Figure S4). Similarly, heterologous antibodies raised against *Trichomonas vaginalis* ASCT (α-*Tv*-ASCT, type 1C) recognized native and purified recombinant *Pb*-ASCT1C in immunoblots (Figure S4). Using spinning-disc immunofluorescence confocal and electron microscopy, we explored the 3D morphology of *Pygsuia* MROs. MitoTracker Orange recognizes an elongated organelle located along the dorsum of the cell subtending the flagellum and typically wraps around the DAPI-stained nucleus (Figures 5A and 5B, red panel, and Figure 5C). Both α-*Tv*-ASCT and α-mSUFCBpep antibodies colocalized with MitoTracker (Figures 5A and 5B, respectively, Figure S4, and Movies S1 and S2).

Transmission electron microscopy of *Pygsuia* revealed an electron-dense double-membrane-bound organelle without canonical cristae similar to those reported in *Breviata anathema* [45] (Figure 5C). Like many other MROs, there is no evidence for an organellar genome since fluorescent nucleic acid dyes such as DAPI and DRAQ5 did not detect nucleic acid inside the organelle (data not shown). Furthermore, we did not identify any genes typically described as organellar genome encoded (such as respiratory chain proteins) or organelle specific transcription- or translation-related proteins (such as RNA polymerase or mitochondrial ribosomal proteins).

## Discussion

Microscopic analysis of *Pygsuia* identified a double-membrane-bound, MitoTracker-reactive structure reminiscent of the hydrogenosomes of *Trichomonas vaginalis.* However, unlike the *T. vaginalis* organelle, the *Pygsuia* MRO is structurally unique and appears to be restricted to one organelle per cell. Next-generation sequence technology has allowed us to characterize the transciptome of *P. biforma* and infer 122 putative MRO proteins, the majority of which have predicted MTS (Figure 1, black outline; Document S2). This unique set of functions predicted for the *Pygsuia* MRO not only bridges the gap between hydrogen-producing mitochondria (HPMs) and hydrogenosomes [46], but also reveals completely novel biochemical properties associated with an MRO.

### Energy Metabolism in MROs

HPMs and hydrogenosomes are ATP- and hydrogen-producing organelles (via SCS, ASCT, and HYDA) that also participate in pyruvate oxidation (via PNO or PDH in HPMs or via PFL or PFO in hydrogenosomes). In these organelles, HYDA function is dependent on H cluster maturation by three HYDA maturases (HYDE, HYDF, and HYDG). We identified putative organellar PFO, HYDA, ASCT, SCS, and all three HYDA maturases in *Pygsuia*. Since we predict dual localization of HYDA in both the MRO (canonical *Pb*-mHYDA) and cytoplasm

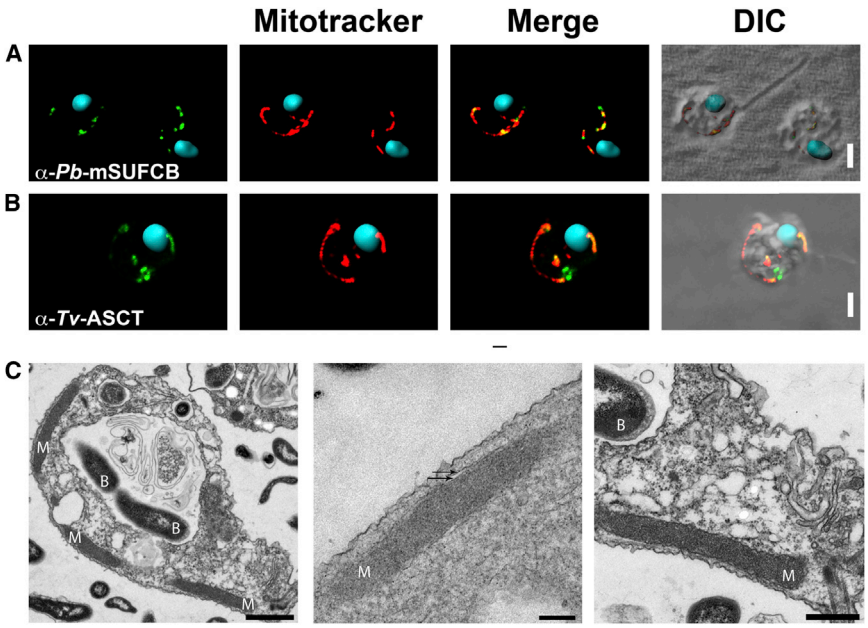


Figure 5. Antibodies Raised against ASCT and SUFCB Localize to *Pygsuia* MROs Using Immunofluorescence Confocal Microscopy

(A and B) mSUFCB (green; A) and ASCT (green; B) colocalized with MitoTracker Orange in *Pygsuia* cells. Confocal slices (0.3 μm) were deconvoluted and combined to render a 3D image. DAPI-stained nuclei (blue) were rendered in Imaris. DIC, differential interference contrast. Scale bars represent 5 μm.

(C) Transmission electron microscopy of *Pygsuia* cells. MRO (M) and food bacteria (B) are labeled. Arrows indicate the presence of a double membrane (middle). Scale bars represent 1000 (left), 200 (middle), and 500 (right) nm.

See also Figure S4 and Movies S1 and S2.

(*Pb*-cHYDA-CysJ1-3 and *Pb*-cSD-HYDA) of *Pygsuia*, it is unclear how the cytoplasmic HYDAs are matured. Either the maturases are dual targeted as described for other proteins in some model systems [47] or the putatively cytosolic hydrogenases can function without maturation. The latter possibility may be related to the presence of additional SD or CYSJ domains on the cytoplasmic hydrogenases.

Similar to the HPMs of *Blastocystis*, *Pygsuia* organelles appear to have an incomplete TCA cycle possessing only FH, CII, and SCS, suggesting that malate is ultimately converted to succinate. In this scenario, CII would function in the reductive reverse direction (as a fumarate reductase) and require a quinone with a lower electron potential, such as RQ [37, 48], and a corresponding RQ reductase. In fact, we identified a gene encoding a recently described RQ biosynthesis enzyme (RQUA [36]) with an MTS in *Pygsuia biforma* and other eukaryotes that appears to have been laterally acquired (Figure 2). The exact pathway for RQ biosynthesis remains elusive; however, recent reports suggest that it can be synthesized from UQ [35, 36]. Since we were unable to identify all the components for ubiquinone biosynthesis, *P. biforma* might rely on exogenous UQ—much like UQ-deficient yeast [49] or humans [50, 51]. Transport of exogenous UQ to mitochondria is not well understood. However, in UQ-deficient mice, exogenously supplied UQ is specifically transported to the IM of the mitochondrion [52]. We hypothesize that a similar transport mechanism could exist in *Pygsuia*, in which bacteria-derived UQ is transported from the food vacuole or plasma membrane to the MRO and specifically incorporated into the IM, where it is converted to RQ.

The MROs of *Pygsuia* seems to blur the boundaries between HPMs and hydrogenosomes since its proteins are predicted to be involved in pyruvate oxidation and hydrogen production like hydrogenomes (PFO, HYDA, ASCT, and SCS), but also HPM features such as quinol reoxidation (CII and AOX, but not CI).

### Conservation of Mitochondrial Protein Import

In eukaryotes, the vast majority of mitochondrial matrix proteins are encoded by the nucleus and are subsequently transported into the organelle [53]. When protein import components are compared across eukaryotic diversity, the complement of proteins identified in *Pygsuia* is similar to that of other non-Opisthokonts (e.g., *Dictyostelium*), with the exception of the outer-membrane complex (*Pygsuia* only encodes TOM40 and SAM50). *Pygsuia* encodes many of the same components as other well-studied MRO-bearing organisms (*T. vaginalis*, *E. histolytica*, and microsporidians [54, 55]), such as SAM50, TOM40, TIM23, TIM17, and PAM complex. The widespread conservation of the aforementioned proteins in otherwise "reduced" MROs from diverse and distantly related organisms suggests that they represent the "core" components of protein import. However, *Pygsuia* appears to have a more elaborate import apparatus compared to other MRO-bearing organisms since it encodes components of the IMS disulfide relay system (TIM8, TIM9, TIM10, TIM13, and MIA40) and Tim50 [55] (Document S2).

### Acquisition of SUF-like Fe-S Cluster Biosynthesis and Loss of ISC Machineries in the *Pygsuia* Lineage

Among eukaryotes, the Archamoebae lineage (i.e., *Entamoeba* and *Mastigamoeba*) was thought to be unique in having lost the organellar ISC system for Fe-S cluster biogenesis and possessing instead a homologous NIF system acquired by LGT from ε-proteobacteria [7, 15, 16]. In some bacteria and these amoebae, the simpler NIF system is the only system present for the synthesis of Fe-S clusters [56]. A recent report demonstrated that *Mastigamoeba balamuthi* actually encodes two copies of each component of the NIF system: two targeted to the MRO (*Mb*-NifS-M and *Mb*-NifU-M) and two destined for the cytoplasm (*Mb*-NifS-C and *Mb*-NifU-C) [15]. Here, we report another apparent loss of the ISC system in *Pygsuia biforma.* The high depth of Illumina sequencing coverage we have obtained for ISC-related genes such as *nfu1* and *ind1* (1596.36× and 243.4×, respectively) suggests that the lack of reads corresponding to any ISC homologs in our *Pygsuia* transcriptome most likely represents genuine absences of the genes. A complete genome sequence for *Pygsuia* would be useful to confirm this observation.

We identified two fused SUFC/SUFB scaffold proteins (SUFCB) in *Pygsuia biforma* and showed that the version possessing a predicted mitochondrial targeting peptide (*Pb*-mSUFCB) is in fact localized to the MROs by immunolocalization in *Pygsuia* (Figures 5 and S5). This SUFCB fusion protein is

also present in *Blastocystis*; however, the gene exists only in single copy, and the protein product was shown to localize to the cytoplasm [17]. Our phylogenetic analyses of SUFCB from *Blastocystis* and *Pygsuia* suggest that the *sufC*/*sufB* operon was acquired by one of these eukaryotic lineages from a Methanomicrobiales archaeon donor and subsequently fused into a single open reading frame in the recipient genome. The *sufCB* fusion gene was then transferred to the other eukaryotic lineage through a eukaryote-to-eukaryote LGT. Since we were unable to identify SUFCB in *Breviata anathema* (and the less sampled *Subulatomonas tetraspora*; Document S2), we suspect that the LGT event happened after the divergence of *Pygsuia* from other breviates. We propose that the *Pygsuia sufCB* was duplicated and that one of the copies eventually acquired a MTS. Over time, the MRO SUFCB system may have functionally replaced the ancestral mitochondrial ISC system, resulting in the loss of all ISC components, including the nuclear transcription factor ISCR.

Unlike the NIF system present in *Mastigamoeba* and *Entamoeba*, the SUF system of *Pygsuia biforma* (SUFCB) is not homologous to any component of ISC. This nonhomologous replacement scenario requires the coevolution of chaperone proteins (NFU1 and IND1) that have to now interact with the SUFCB proteins in order to transfer the Fe-S clusters to apoproteins. This hypothesis is consistent with the observation that, in bacteria that harbor ISC and SUF systems (e.g., *E. coli*), the typically ISC-associated NFU1 has been shown to transfer Fe-S clusters from $SUFBC_2D$ to apoproteins [57]. As with the SUFCB proteins of *Blastocystis* and methanomicrobiales, we were unable to identify the residues responsible for binding flavin in the *Pygsuia biforma* SUFCB sequences. The flavin cofactor of the *E. coli* $SUFBC_2D$ complex has been hypothesized to be important for the acquisition of ferric iron from various iron donors (ferritin, ferric citrate, and frataxin) [41]. However, lack of flavin binding does not prevent removal of the Fe-S cluster from the $SUFBC_2D$ complex of *E. coli* [58]. Moreover, ferritin and frataxin have not been identified in *Pygsuia*. Therefore, the apparent absence of the flavin binding residues of the SUFCB proteins of *Pygsuia*, *Blastocystis*, and Methanomicrobiales might be related to the absence of such electron-dependent iron donors. The source and means by which the SUFCB proteins of these organisms acquire iron remains unknown. Similarly, the traditional components of the *suf* operon (*sufA-E* and *sufS*) have not been identified in *Pygsuia*, *Blastocystis*, and some archaea, suggesting that these organisms employ a yet unknown process of Fe-S cluster biosynthesis.

It is unclear why an ISC system would be replaced by the nonhomologous SUF system in the *Pygsuia* MRO. Clearly, after acquisition of the SUF system by LGT, the ancestral breviate must have possessed both Fe-S biosynthetic systems. The *suf* operon in prokaryotes is typically upregulated under (and more tolerant to) iron starvation and oxidative stress [59]. If the ancestor of *Pygsuia* was periodically exposed to such conditions, this could have favored the maintenance of the acquired SUF system over the ancestral ISC system.

## Conclusions

Here we report a unique collection of functions associated with the mitochondrion-related organelles of the breviate flagellate *Pygsuia biforma.* In addition to the typical MRO and mitochondrial processes, we identified genes involved in functions previously unknown in mitochondria or MROs. Some of these genes were most likely acquired by LGT, including those encoding a rhodoquinone biosynthesis enzyme and a SUFCB protein involved in Fe-S cluster biosynthesis. These are striking examples of how lateral gene transfer can remodel MRO function in adaptation to hypoxia.

As more mitochondria and MROs are characterized from a greater diversity of eukaryotic lineages, it is becoming clear that at least one kind of Fe-S cluster biosynthesis system is essential. While most eukaryotes have retained the ISC system in their MROs, the two clear exceptions are the MROs of the Archamoeba *Mastigamoeba* that has a NIF system and the MROs of *Pygsuia biforma* that have SUF system. This strongly suggests that the reactions needed for the synthesis of Fe-S clusters, regardless of their evolutionary origin, demand compartmentalization. This further highlights the fundamental role and widespread conservation of Fe-S cluster biosynthesis in mitochondria and MROs.

The novel combination of properties of the *Pygsuia* organelles cannot be easily fit into any of the classes of MRO functions recently proposed by Müller and colleagues [46]. As more lineages of anaerobic/microaerophilic protists are studied, the diversity of MRO properties will most likely increase, suggestive of a continuous spectrum of metabolic phenotypes rather than well-defined classes and revealing the plasticity of these endosymbiont-derived organelles.

### Accession Numbers

The GenBank dbEST accession numbers for the *Breviata anathema* data reported in this paper are JZ547815–JZ554760.

### Supplemental Information

Supplemental Information includes four figures, Supplemental Results, Supplemental Experimental Procedures, gene and protein information, phylogenies, and two movies and can be found with this article online at http://dx.doi.org/10.1016/j.cub.2014.04.033.

### Acknowledgments

C.S. is supported by a Natural Science and Engineering Research Council (NSERC) Alexander Graham Bell Canadian Graduate Scholarship and Killam Graduate Scholarship. L.E. and M.B. were supported by Centre for Comparative Genomics and Evolutionary Bioinformatics postdoctoral fellowships from the Tula Foundation. The majority of this work was supported by a Canadian Institutes of Health Research Grant (CIHR; MOP-82809) awarded to A.J.R. A.J.R. acknowledges the Canadian Institute for Advanced Research Program in Microbial Biodiversity, in which he is a Senior Fellow, and the Canada Research Chairs Program. Work in G.D.'s laboratory was supported by a CIHR Operating Grant (MOP-84260) and a Discovery Grant from the NSERC. G.D. is also a senior scientist of the Beatrice Hunter Cancer Research Institute (BHCRI; Halifax) and a CIHR New Investigator. Work in M.v.d.G.'s laboratory was supported by a CoSyst-BBSRC grant. The authors would also like to thank Melanie Dobson and Barbara Karten for providing reagents and advice for various experiments and A.G.M. Tielens for providing the $\alpha$-*Tv*ASCT antibodies, the Mississippi State University's High Performance Computing Collaboratory for computational resources, and Dale Corkery for assistance with microscopy.

Received: February 12, 2014
Revised: April 8, 2014
Accepted: April 15, 2014
Published: May 22, 2014

### References

1. Gray, M.W., Burger, G., and Lang, B.F. (2001). The origin and early evolution of mitochondria. Genome Biol. *2*, S1018.
2. Kita, K., Takamiya, S., Furushima, R., Ma, Y.C., Suzuki, H., Ozawa, T., and Oya, H. (1988). Electron-transfer complexes of Ascaris suum

muscle mitochondria. III. Composition and fumarate reductase activity of complex II. Biochim. Biophys. Acta *935*, 130–140.
3. Steinbüchel, A., and Müller, M. (1986). Anaerobic pyruvate metabolism of Tritrichomonas foetus and Trichomonas vaginalis hydrogenosomes. Mol. Biochem. Parasitol. *20*, 57–65.
4. van Grinsven, K.W.A., Rosnowsky, S., van Weelden, S.W.H., Pütz, S., van der Giezen, M., Martin, W., van Hellemond, J.J., Tielens, A.G.M., and Henze, K. (2008). Acetate:succinate CoA-transferase in the hydrogenosomes of Trichomonas vaginalis: identification and characterization. J. Biol. Chem. *283*, 1411–1418.
5. Tovar, J., León-Avila, G., Sánchez, L.B., Sutak, R., Tachezy, J., van der Giezen, M., Hernández, M., Müller, M., and Lucocq, J.M. (2003). Mitochondrial remnant organelles of Giardia function in iron-sulphur protein maturation. Nature *426*, 172–176.
6. Reeves, R.E., Warren, L.G., Susskind, B., and Lo, H.S. (1977). An energy-conserving pyruvate-to-acetate pathway in Entamoeba histolytica. Pyruvate synthase and a new acetate thiokinase. J. Biol. Chem. *252*, 726–731.
7. Gill, E.E., Diaz-Triviño, S., Barberà, M.J., Silberman, J.D., Stechmann, A., Gaston, D., Tamas, I., and Roger, A.J. (2007). Novel mitochondrion-related organelles in the anaerobic amoeba Mastigamoeba balamuthi. Mol. Microbiol. *66*, 1306–1320.
8. Stechmann, A., Hamblin, K., Pérez-Brocal, V., Gaston, D., Richmond, G.S., van der Giezen, M., Clark, C.G., and Roger, A.J. (2008). Organelles in Blastocystis that blur the distinction between mitochondria and hydrogenosomes. Curr. Biol. *18*, 580–585.
9. Barberà, M.J., Ruiz-Trillo, I., Tufts, J.Y.A., Bery, A., Silberman, J.D., and Roger, A.J. (2010). Sawyeria marylandensis (Heterolobosea) has a hydrogenosome with novel metabolic properties. Eukaryot. Cell *9*, 1913–1924.
10. Zubáčová, Z., Novák, L., Bublíková, J., Vacek, V., Fousek, J., Rídl, J., Tachezy, J., Doležal, P., Vlček, C., and Hampl, V. (2013). The mitochondrion-like organelle of Trimastix pyriformis contains the complete glycine cleavage system. PLoS ONE *8*, e55417.
11. Burki, F., Corradi, N., Sierra, R., Pawlowski, J., Meyer, G.R., Abbott, C.L., and Keeling, P.J. (2013). Phylogenomics of the intracellular parasite Mikrocytos mackini reveals evidence for a mitosome in rhizaria. Curr. Biol. *23*, 1541–1547.
12. Stechmann, A., Baumgartner, M., Silberman, J.D., and Roger, A.J. (2006). The glycolytic pathway of Trimastix pyriformis is an evolutionary mosaic. BMC Evol. Biol. *6*, 101.
13. Stehling, O., and Lill, R. (2013). The role of mitochondria in cellular iron-sulfur protein biogenesis: mechanisms, connected processes, and diseases. Cold Spring Harb. Perspect. Biol. *5*, a011312.
14. Takahashi, Y., and Tokumoto, U. (2002). A third bacterial system for the assembly of iron-sulfur clusters with homologs in archaea and plastids. J. Biol. Chem. *277*, 28380–28383.
15. Nývltová, E., Šuták, R., Harant, K., Šedinová, M., Hrdy, I., Paces, J., Vlček, C., and Tachezy, J. (2013). NIF-type iron-sulfur cluster assembly system is duplicated and distributed in the mitochondria and cytosol of Mastigamoeba balamuthi. Proc. Natl. Acad. Sci. USA *110*, 7371–7376.
16. van der Giezen, M., Cox, S., and Tovar, J. (2004). The iron-sulfur cluster assembly genes iscS and iscU of Entamoeba histolytica were acquired by horizontal gene transfer. BMC Evol. Biol. *4*, 7.
17. Tsaousis, A.D., Ollagnier de Choudens, S., Gentekaki, E., Long, S., Gaston, D., Stechmann, A., Vinella, D., Py, B., Fontecave, M., Barras, F., et al. (2012). Evolution of Fe/S cluster biogenesis in the anaerobic parasite Blastocystis. Proc. Natl. Acad. Sci. USA *109*, 10426–10431.
18. Brown, M.W., Sharpe, S.C., Silberman, J.D., Heiss, A.A., Lang, B.F., Simpson, A.G.B., and Roger, A.J. (2013). Phylogenomics demonstrates that breviate flagellates are related to opisthokonts and apusomonads. Proc. Biol. Sci. *280*, 20131755.
19. Smith, A.C., Blackshaw, J.A., and Robinson, A.J. (2012). MitoMiner: a data warehouse for mitochondrial proteomics data. Nucleic Acids Res. *40* (Database issue), D1160–D1167.
20. Emanuelsson, O., Nielsen, H., Brunak, S., and von Heijne, G. (2000). Predicting subcellular localization of proteins based on their N-terminal amino acid sequence. J. Mol. Biol. *300*, 1005–1016.
21. Claros, M.G., and Vincens, P. (1996). Computational method to predict mitochondrially imported proteins and their targeting sequences. Eur. J. Biochem. *241*, 779–786.
22. Grant, J. R., Lahr, D. J. G., Rey, F. E., Burleigh, J. G., Gordon, J. I., Knight, R., Molestina, R. E., and Katz, L. A. Gene discovery from a pilot study of the transcriptomes from three diverse microbial eukaryotes: Corallomyxa tenera, Chilodonella uncinata, and Subulatomonas tetraspora. Protist Genomics *1*, 3–18.
23. Bricker, D.K., Taylor, E.B., Schell, J.C., Orsak, T., Boutron, A., Chen, Y.-C., Cox, J.E., Cardon, C.M., Van Vranken, J.G., Dephoure, N., et al. (2012). A mitochondrial pyruvate carrier required for pyruvate uptake in yeast, Drosophila, and humans. Science *337*, 96–100.
24. Ochoa, S., Mehler, A.H., and Kornberg, A. (1948). Biosynthesis of dicarboxylic acids by carbon dioxide fixation; isolation and properties of an enzyme from pigeon liver catalyzing the reversible oxidative decarboxylation of 1-malic acid. J. Biol. Chem. *174*, 979–1000.
25. de Graaf, R.M., Ricard, G., van Alen, T.A., Duarte, I., Dutilh, B.E., Burgtorf, C., Kuiper, J.W.P., van der Staay, G.W.M., Tielens, A.G.M., Huynen, M.A., and Hackstein, J.H. (2011). The organellar genome and metabolic potential of the hydrogen-producing mitochondrion of Nyctotherus ovalis. Mol. Biol. Evol. *28*, 2379–2391.
26. Hug, L.A., Stechmann, A., and Roger, A.J. (2010). Phylogenetic distributions and histories of proteins involved in anaerobic pyruvate metabolism in eukaryotes. Mol. Biol. Evol. *27*, 311–324.
27. Stairs, C.W., Roger, A.J., and Hampl, V. (2011). Eukaryotic pyruvate formate lyase and its activating enzyme were acquired laterally from a Firmicute. Mol. Biol. Evol. *28*, 2087–2099.
28. Atteia, A., van Lis, R., Gelius-Dietrich, G., Adrait, A., Garin, J., Joyard, J., Rolland, N., and Martin, W. (2006). Pyruvate formate-lyase and a novel route of eukaryotic ATP synthesis in Chlamydomonas mitochondria. J. Biol. Chem. *281*, 9909–9918.
29. Akhmanova, A., Voncken, F.G., Hosea, K.M., Harhangi, H., Keltjens, J.T., op den Camp, H.J., Vogels, G.D., and Hackstein, J.H. (1999). A hydrogenosome with pyruvate formate-lyase: anaerobic chytrid fungi use an alternative route for pyruvate catabolism. Mol. Microbiol. *32*, 1103–1114.
30. Bui, E.T., and Johnson, P.J. (1996). Identification and characterization of [Fe]-hydrogenases in the hydrogenosome of Trichomonas vaginalis. Mol. Biochem. Parasitol. *76*, 305–310.
31. Mulder, D.W., Boyd, E.S., Sarma, R., Lange, R.K., Endrizzi, J.A., Broderick, J.B., and Peters, J.W. (2010). Stepwise [FeFe]-hydrogenase H-cluster assembly revealed in the structure of HydA(DeltaEFG). Nature *465*, 248–251.
32. Vanlerberghe, G.C., and McIntosh, L. (1997). Alternative oxidase: from gene to function. Annu. Rev. Plant Physiol. Plant Mol. Biol. *48*, 703–734.
33. Ansell, R., Granath, K., Hohmann, S., Thevelein, J.M., and Adler, L. (1997). The two isoenzymes for yeast NAD+-dependent glycerol 3-phosphate dehydrogenase encoded by GPD1 and GPD2 have distinct roles in osmoadaptation and redox regulation. EMBO J. *16*, 2179–2187.
34. Iwata, F., Shinjyo, N., Amino, H., Sakamoto, K., Islam, M.K., Tsuji, N., and Kita, K. (2008). Change of subunit composition of mitochondrial complex II (succinate-ubiquinone reductase/quinol-fumarate reductase) in Ascaris suum during the migration in the experimental host. Parasitol. Int. *57*, 54–61.
35. Brajcich, B.C., Iarocci, A.L., Johnstone, L.A., Morgan, R.K., Lonjers, Z.T., Hotchko, M.J., Muhs, J.D., Kieffer, A., Reynolds, B.J., Mandel, S.M., et al. (2010). Evidence that ubiquinone is a required intermediate for rhodoquinone biosynthesis in Rhodospirillum rubrum. J. Bacteriol. *192*, 436–445.
36. Lonjers, Z.T., Dickson, E.L., Chu, T.-P.T., Kreutz, J.E., Neacsu, F.A., Anders, K.R., and Shepherd, J.N. (2012). Identification of a new gene required for the biosynthesis of rhodoquinone in Rhodospirillum rubrum. J. Bacteriol. *194*, 965–971.
37. Hoffmeister, M., van der Klei, A., Rotte, C., van Grinsven, K.W.A., van Hellemond, J.J., Henze, K., Tielens, A.G.M., and Martin, W. (2004). Euglena gracilis rhodoquinone:ubiquinone ratio and mitochondrial proteome differ under aerobic and anaerobic conditions. J. Biol. Chem. *279*, 22422–22429.
38. Hrdy, I., Hirt, R.P., Dolezal, P., Bardonová, L., Foster, P.G., Tachezy, J., and Embley, T.M. (2004). Trichomonas hydrogenosomes contain the NADH dehydrogenase module of mitochondrial complex I. Nature *432*, 618–622.
39. Milenkovic, D., Ramming, T., Müller, J.M., Wenz, L.-S., Gebert, N., Schulze-Specking, A., Stojanovski, D., Rospert, S., and Chacinska, A. (2009). Identification of the signal directing Tim9 and Tim10 into the intermembrane space of mitochondria. Mol. Biol. Cell *20*, 2530–2539.
40. Lill, R. (2009). Function and biogenesis of iron-sulphur proteins. Nature *460*, 831–838.

41. Roche, B., Aussel, L., Ezraty, B., Mandin, P., Py, B., and Barras, F. (2013). Iron/sulfur proteins biogenesis in prokaryotes: formation, regulation and diversity. Biochim. Biophys. Acta *1827*, 455–469.
42. Jiang, D., Zhao, L., Clish, C.B., and Clapham, D.E. (2013). Letm1, the mitochondrial Ca2+/H+ antiporter, is essential for normal glucose metabolism and alters brain function in Wolf-Hirschhorn syndrome. Proc. Natl. Acad. Sci. USA *110*, E2249–E2254.
43. Arkblad, E.L., Egorov, M., Shakhparonov, M., Romanova, L., Polzikov, M., and Rydström, J. (2002). Expression of proton-pumping nicotinamide nucleotide transhydrogenase in mouse, human brain and C. elegans. Comp. Biochem. Physiol. B Biochem. Mol. Biol. *133*, 13–21.
44. Tian, H.-F., Feng, J.-M., and Wen, J.-F. (2012). The evolution of cardiolipin biosynthesis and maturation pathways and its implications for the evolution of eukaryotes. BMC Evol. Biol. *12*, 32.
45. Heiss, A.A., Walker, G., and Simpson, A.G.B. (2013). The flagellar apparatus of Breviata anathema, a eukaryote without a clear supergroup affinity. Eur. J. Protistol. *49*, 354–372.
46. Müller, M., Mentel, M., van Hellemond, J.J., Henze, K., Woehle, C., Gould, S.B., Yu, R.-Y., van der Giezen, M., Tielens, A.G.M., and Martin, W.F. (2012). Biochemistry and evolution of anaerobic energy metabolism in eukaryotes. Microbiol. Mol. Biol. Rev. *76*, 444–495.
47. Baudisch, B., Langner, U., Garz, I., and Klösgen, R.B. (2014). The exception proves the rule? Dual targeting of nuclear-encoded proteins into endosymbiotic organelles. New Phytol. *201*, 80–90.
48. Amino, H., Osanai, A., Miyadera, H., Shinjyo, N., Tomitsuka, E., Taka, H., Mineki, R., Murayama, K., Takamiya, S., Aoki, T., et al. (2003). Isolation and characterization of the stage-specific cytochrome b small subunit (CybS) of Ascaris suum complex II from the aerobic respiratory chain of larval mitochondria. Mol. Biochem. Parasitol. *128*, 175–186.
49. Padilla-López, S., Jiménez-Hidalgo, M., Martín-Montalvo, A., Clarke, C.F., Navas, P., and Santos-Ocaña, C. (2009). Genetic evidence for the requirement of the endocytic pathway in the uptake of coenzyme Q6 in Saccharomyces cerevisiae. Biochim. Biophys. Acta *1788*, 1238–1248.
50. Lagier-Tourenne, C., Tazir, M., López, L.C., Quinzii, C.M., Assoum, M., Drouot, N., Busso, C., Makri, S., Ali-Pacha, L., Benhassine, T., et al. (2008). ADCK3, an ancestral kinase, is mutated in a form of recessive ataxia associated with coenzyme Q10 deficiency. Am. J. Hum. Genet. *82*, 661–672.
51. Quinzii, C.M., and Hirano, M. (2010). Coenzyme Q and mitochondrial disease. Dev. Disabil. Res. Rev. *16*, 183–188.
52. Lapointe, J., Wang, Y., Bigras, E., and Hekimi, S. (2012). The submitochondrial distribution of ubiquinone affects respiration in long-lived Mclk1+/- mice. J. Cell Biol. *199*, 215–224.
53. Dolezal, P., Likic, V., Tachezy, J., and Lithgow, T. (2006). Evolution of the molecular machines for protein import into mitochondria. Science *313*, 314–318.
54. Heinz, E., and Lithgow, T. (2013). Back to basics: a revealing secondary reduction of the mitochondrial protein import pathway in diverse intracellular parasites. Biochim. Biophys. Acta *1833*, 295–303.
55. Liu, Z., Li, X., Zhao, P., Gui, J., Zheng, W., and Zhang, Y. (2011). Tracing the evolution of the mitochondrial protein import machinery. Comput. Biol. Chem. *35*, 336–340.
56. Olson, J.W., Agar, J.N., Johnson, M.K., and Maier, R.J. (2000). Characterization of the NifU and NifS Fe-S cluster formation proteins essential for viability in Helicobacter pylori. Biochemistry *39*, 16213–16219.
57. Py, B., Gerez, C., Angelini, S., Planel, R., Vinella, D., Loiseau, L., Talla, E., Brochier-Armanet, C., Garcia Serres, R., Latour, J.-M., et al. (2012). Molecular organization, biochemical function, cellular role and evolution of NfuA, an atypical Fe-S carrier. Mol. Microbiol. *86*, 155–171.
58. Wollers, S., Layer, G., Garcia-Serres, R., Signor, L., Clemancey, M., Latour, J.-M., Fontecave, M., and Ollagnier de Choudens, S. (2010). Iron-sulfur (Fe-S) cluster assembly: the SufBCD complex is a new type of Fe-S scaffold with a flavin redox cofactor. J. Biol. Chem. *285*, 23331–23341.
59. Outten, F.W., Djaman, O., and Storz, G. (2004). A suf operon requirement for Fe-S cluster assembly during iron starvation in Escherichia coli. Mol. Microbiol. *52*, 861–872.